

Linear stability test for Hamiltonian orbits

Susan J. Feingold* and Asher Peres

Department of Physics, Technion-Israel Institute of Technology, 32000 Haifa, Israel

(Received 13 November 1981)

The following test can distinguish regular from irregular orbits, even in marginal cases. A small sphere in phase space, initially centered at the starting point of the orbit, evolves into an ellipsoid by virtue of the Hamiltonian equations of motion. This ellipsoid rotates and vibrates "erratically" as its center moves along the classical trajectory. However, the proposed test involves only consecutive shapes of the ellipsoid as the orbit happens to pass in the vicinity of its initial point. The major axis of the ellipsoid then increases with time in a way which is roughly linear for regular orbits, and roughly exponential for irregular ones. Moreover, if the orbit is regular, the behavior of the angle between the major axis and the tangent to the trajectory indicates the smoothness of the invariant torus containing the orbit. This angle tends to a constant if the torus is very smooth, and oscillates if the torus has a complicated shape in the vicinity of the initial point.

I. INTRODUCTION

The stability of classical orbits is a problem of paramount importance in many applications, such as celestial mechanics, high-energy accelerators, magnetic fusion and also, in the light of the correspondence principle, in molecular physics.¹⁻³ It is well known that there are two types of classical Hamiltonian orbits for a system with N degrees of freedom.⁴ If there are N isolating constants of the motion, the orbits lie on N -dimensional tori in phase space and are called "regular." They are multiply periodic in time and a cluster of points placed on neighboring orbits spreads at a rate which is roughly linear in time. Otherwise the orbits are "irregular" or "chaotic" (possibly ergodic) and the rate of divergence of neighboring orbits is roughly exponential.

In a strict mathematical sense, all these nondissipative orbits are "unstable" because they do not tend to an equilibrium position.⁵ However, the difference between linear and exponential instability is crucial. As the irregular orbits are not constrained to lie on N -dimensional tori, the points which belonged to the initial cluster will be found, after a finite time, arbitrarily close to *any* point of the accessible region of phase space. This "mixing" behavior is usually construed as the rationale for irreversibility in statistical physics.

Unfortunately, it is in general very difficult to prove the existence or nonexistence of $N - 1$ isolating constants of the motion, in addition to the Hamiltonian. They may be formally constructed by perturbation methods,⁶ but the convergence of

the perturbation series is problematic. Early investigations appeared to indicate that the series converged in some parts of phase space and diverged in others,⁷ but there was no satisfactory method for determining the domain of convergence or the onset of stochasticity.⁸ It is known today that there are in fact small irregular regions arbitrarily close to any point of a regular region.⁹ These small stochastic regions are trapped between invariant tori and very precise calculations are required to find them (an example will be given below). It may also happen that a trajectory just beyond the boundary of the regular domain may remain there for a long period of time before disclosing its chaotic nature.^{10,11} Strictly speaking, no numerical experiment can ever prove the existence of invariant tori,¹² because it is always conceivable that high-order iterates may diverge from the torus suggested by earlier iterates. Conversely, it may happen that there is a method in what may seem to be chaos and points which look random actually do lie on some definite but very complicated torus.

However, *periodic* orbits, which form a set of measure zero, allow a mathematically meaningful formulation of the problem.¹³ Intuitively, the idea is to consider a trajectory passing very close to a fixed point (i.e., a point lying on a periodic orbit). This trajectory will return periodically very close to that point. We can then observe whether, after an integral number of periods, the "distance" from the fixed point increases linearly or exponentially (or otherwise). In this paper, we seek a suitable modification of this method which can be used to determine the stability of a given *nonperiodic* tra-

jectory.

Conceptually, we could seek a fixed point not too far from the given trajectory, which is always possible in principle.¹⁴ Indeed, for most Hamiltonian systems, the periodic solutions are “dense” among all bounded solutions. This in turn allows all bounded solutions to be approximated arbitrarily well by periodic solutions.¹⁵ Unfortunately, this approach is rarely practical, because a good approximation usually requires a period which is inordinately long (a Poincaré recurrence).

On the other hand, if we attempt a straightforward generalization of the above method by following the entire time behavior of small deviations from arbitrary nonperiodic orbits, another difficulty appears. The “distance” between neighboring orbits does not increase monotonically, but fluctuates wildly as it increases.^{16,17} Although a limiting behavior can in principle be defined,¹⁸ the time necessary to attain it may be so long that an answer cannot be given.¹⁹

In this article we propose a new, efficient method to distinguish regular from irregular orbits, including marginal cases such as small stochastic domains trapped within regular tori. The idea is to consider the evolution of a small domain of phase space, which is initially an infinitesimal “sphere” centered at the starting point of the orbit. As time passes, this sphere becomes an ellipsoid which rotates and vibrates erratically while its center moves along the orbit. Now, if the orbit were periodic, it would be enough to consider consecutive shapes of the ellipsoid as its center passes through a fixed point in order to have an unambiguous stability criterion. For a nonperiodic orbit we intuitively expect, and our numerical calculations confirm, that a similar stability criterion is obtained by considering successive shapes of the ellipsoid as its center passes in the *vicinity* of the initial point of the orbit. If the orbit is regular, the major axis increases almost linearly with time, otherwise it increases almost exponentially. The large fluctuations mentioned above do *not* appear if we consider only points of the orbit which are reasonably close to the initial point.

Another interesting indicator is the “angle” between the major axis of the ellipsoid and the tangent to a regular orbit. This angle tends to a constant if the invariant torus is very smooth, and oscillates if the torus has a complicated shape in the vicinity of the initial point.

In Sec. II of this paper, we discuss the equations of motion of the ellipsoid and show why we expect

its elongation to behave about linearly or exponentially in time when the center of the ellipsoid is close to the initial point. In Sec. III, we illustrate these equations of motion by numerical calculations for several orbits of the Hénon-Heiles model.²⁰ Finally in Sec. IV, we compare various known tests of stability, in particular, when the latter is marginal.

However, before we proceed with the calculations, we still must explain why we wrote geometric terms such as distance, sphere, angle, etc., using quotation marks. The reason is that phase space has no metric structure²¹ and the distance between two points which grows with time, linearly or exponentially, cannot be a concept invariant under canonical transformations. Nevertheless, as will be seen in the next section, the *asymptotic rate of growth* of the distance is canonically invariant. It is not affected by the arbitrariness of the Euclidean metric which we introduce in phase space.

It is, in fact, possible to reformulate our test in a canonically invariant way, without using any Euclidean metric (see Appendix B). We prefer, however, the geometrically intuitive approach used below.

II. LINEARIZED EQUATIONS OF MOTION

Some parts of this section are not new, but are included in order to define the notation and for the sake of completeness. We consider a Hamiltonian $H(\vec{r})$ where \vec{r} is the “vector” with components $q_1 \cdots q_n, p_1 \cdots p_n$. The equations of motion are

$$\dot{r}_i = \eta_{ij} \left[\frac{\partial H}{\partial r_j} \right], \quad (1)$$

where η_{ij} is the symplectic matrix

$$\eta_{ij} = -\eta_{ji} = \delta_{i+n,j}, \quad (2)$$

and repeated indices imply summation, as usual.

To test the stability of the orbit given by (1), we consider an infinitesimal deviation $r_i \rightarrow r_i + \epsilon \rho_i$ and linearize (1), to obtain

$$\dot{\rho}_i = \eta_{ij} \left[\frac{\partial^2 H}{\partial r_j \partial r_k} \right] \rho_k \equiv M_{ik} \rho_k. \quad (3)$$

It is well known that linearized stability is only an approximation and may lack some essential features of the full nonlinear problem.⁵ However, it is a very expedient and usually reliable means to as-

sess the properties of a physical system.

Note that

$$\text{Tr}M=0, \quad (4)$$

and

$$\eta M = -\tilde{M}\eta, \quad (5)$$

where the tilde denotes the transposed matrix. The antisymmetric part of M rotates the vector $\vec{\rho}$ and the symmetric part stretches and compresses $\vec{\rho}$.

After a time t , we obtain

$$\vec{\rho}(t) = S(t)\vec{\rho}(0), \quad (6)$$

where the transfer matrix $S(t)$ satisfies

$$\dot{S} = MS, \quad (7)$$

and $S(0) = I$. We have

$$\frac{d(\text{Det}S)}{dt} = (\text{Det}S)\text{Tr}(S^{-1}\dot{S}) = 0, \quad (8)$$

by virtue of (7) and (4), so that

$$\text{Det}S = 1 \quad (9)$$

is constant. This is Liouville's theorem. Moreover, if we denote by $\tilde{\rho}$ the transposed (row vector) of $\vec{\rho}$, we have

$$\frac{d(\tilde{\rho}_1\eta\tilde{\rho}_2)}{dt} = \tilde{\rho}_1(\tilde{M}\eta + \eta M)\tilde{\rho}_2 = 0, \quad (10)$$

by virtue of (3) and (5). Therefore

$$\tilde{\rho}_1\tilde{S}\eta S\tilde{\rho}_2 = \tilde{\rho}_1\eta\tilde{\rho}_2 \quad (11)$$

for any $\vec{\rho}_1$ and $\vec{\rho}_2$ and it follows that

$$\tilde{S}\eta S = \eta, \quad (12)$$

so that S belongs to the symplectic group.²² It then follows (see Appendix A) that the eigenvalues of S are paired as λ and λ^{-1} and in particular complex eigenvalues lie on the unit circle. This property is important at the boundary between regular and irregular regions, as will be shown below.

Had we chosen a different canonical system, the new components of $\vec{\rho}$ would be linear combinations of the old ones, and therefore the new S matrix would be related to the old one by a *similarity transformation*. This cannot affect the eigenvalues λ , which are canonical invariants at each point of phase space.

Consider now the special case of a periodic orbit, and let S denote the transfer matrix for one complete period. The transfer matrix for n periods is S^n and its eigenvalues are λ^n . If some $|\lambda|$ is larger than 1, the corresponding eigenvector grows

exponentially with the number of periods. If $|\lambda| < 1$, it is paired with $|\lambda^{-1}| > 1$, so that one eigenvector is growing as the other is shrinking. On the other hand, if $\lambda = e^{i\theta}$, the corresponding eigenvector will have its phase rotated but will not grow.

It thus seems surprising that we may also have a *linear growth law*. The latter arises because $\lambda = 1$ is a *doubly degenerate* eigenvalue of S , whenever a periodic orbit passes through its initial point. This can be shown as follows. First, we note that $\rho_i = \dot{r}_i$ is a trivial solution of (3), corresponding to two points moving on the *same* orbit, separated by an infinitesimal time interval ϵ . Therefore for a complete period we have $S d\vec{r}/dt = d\vec{r}/dt$, so that indeed $\lambda = 1$ is an eigenvalue. This eigenvalue must be doubly degenerate, because the product of all eigenvalues is $\text{Det}S = 1$ and all the other eigenvalues are paired as λ and λ^{-1} .

The crucial property of this doubly degenerate eigenvalue is that it has only a *single* eigenvector (namely $\vec{\rho} = d\vec{r}/dt$). As a simple illustration of this property, consider the symplectic matrix

$$C(a) = \begin{pmatrix} 1 & a \\ 0 & 1 \end{pmatrix}. \quad (13)$$

It has a degenerate eigenvalue $\lambda = 1$ and the *only* corresponding eigenvector is

$$\vec{v} = \begin{pmatrix} 1 \\ 0 \end{pmatrix}. \quad (14)$$

Note that

$$C(a)C(b) = C(a+b) \quad (15)$$

and, in particular,

$$[C(a)]^n = C(na), \quad (16)$$

so that one of the matrix elements indeed grows *linearly* with n .

If we introduce the conjugate vector $\vec{u} = \eta\vec{v}$, we have

$$C(a)\vec{u} = \vec{u} - a\vec{v}, \quad (17)$$

or more generally,

$$[C(a)]^n(x\vec{u} + y\vec{v}) = x\vec{u} + (y - nax)\vec{v}. \quad (18)$$

We see that repeated applications of $C(a)$ do *not* affect the \vec{u} component, but the \vec{v} component increases *linearly*. The same property naturally holds for higher dimensional symplectic matrices, *unless there is an additional degeneracy*. For example, if the unit eigenvalue is fourfold degenerate,

the corresponding eigenvector may grow quadratically with time, etc. Although such a degeneracy would normally be considered as accidental, it does happen at the transition from regular to irregular regions, when $\lambda + \lambda^{-1}$, which must be real as shown in Appendix A, grows from $2 - \epsilon$ to $2 + \epsilon$ (see Fig. 1).

We now consider, instead of a single vector $\vec{\rho}$, all the vectors initially lying on a unit sphere $(\vec{\rho}_0)^2 = 1$. After a time t , this sphere becomes an ellipsoid $\vec{\rho} B \vec{\rho} = 1$, where

$$B = \tilde{S}^{-1} S^{-1} \quad (19)$$

by Eq. (6). The eigenvalues of the symmetric matrix B are the inverse squares of the ellipsoid semiaxes. It is thus more convenient to consider

$$A = B^{-1} = S \tilde{S}, \quad (20)$$

which satisfies the equations of motion

$$\dot{A} = MA + A\tilde{M}, \quad (21)$$

because of Eq. (7). Note that $\text{Det} A = 1$, by Eq. (9). We could have reduced by one the dimensionality of the ellipsoid, by considering only its intersection with the energy surface, but this would mar the simplicity of Eq. (21).

To characterize the aspect ratio of the ellipsoid we may compute its major axis, but it is much easier, and almost equivalent, to consider

$$\text{Tr} A = \sum (S_{ij})^2, \quad (22)$$

which is the sum of the squares of the semiaxes, because one of the axes will become considerably longer than all the others. From the preceding argument, we thus expect that for large t

$$(\text{Tr} A)^{1/2} / t \rightarrow \alpha. \quad (23)$$

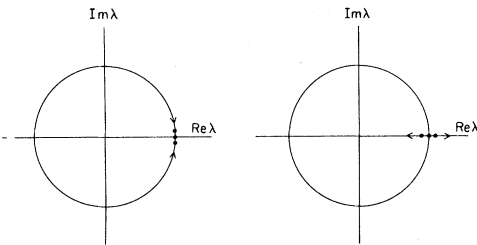


FIG. 1. Confluence of eigenvalues for marginally stable (left) or unstable (right) periodic orbits. The four neighboring eigenvalues of the transfer matrix are 1, 1, and $\exp(\pm i\epsilon)$ or $\exp(\pm\epsilon)$, respectively. The arrows indicate the transition from regularity to stochasticity. Other eigenvalues (for $N > 2$ degrees of freedom) have not been shown.

if the orbit is regular, and

$$\ln(\text{Tr} A) / t \rightarrow \beta, \quad (24)$$

if it is chaotic. The coefficient β is equal to twice the sum of the positive Lyapunov characteristic numbers,^{18,19} also called KSS entropy.²³

The limiting values (23) and (24) are attained *very slowly* for nonperiodic orbits, if the values of t are sampled at arbitrary constant intervals. However, as will be shown in Sec. III, if we consider the ellipsoid only when its center passes in the vicinity of the original point, the convergence of (23) and (24) is quite rapid.

Another interesting question is whether the elongation of the ellipsoid is mostly longitudinal (parallel to the tangent to the orbit in phase space) or transverse. For a regular orbit the argument leading to Eq. (18) shows that the linear growth of $\vec{\rho}$ is parallel to the invariant eigenvector $\vec{v} = d\vec{r}/dt$ because the other eigenvectors are only multiplied by phase factors $\lambda = e^{i\theta}$. One is thus tempted to infer that the points in the ellipsoid spread only in a direction parallel to $d\vec{r}/dt$ and that there is no spreading in directions orthogonal to $d\vec{r}/dt$. However, this is a fallacy because the transfer matrix S is not symmetric but symplectic, and its eigenvectors are *not* orthogonal with respect to the Euclidean metric which we introduced to define a sphere, etc. When a vector $\vec{\rho}$ which is "orthogonal" to $d\vec{r}/dt$ is written as a linear combination of eigenvectors of S , it usually has a component *along* $d\vec{r}/dt$, and therefore will grow linearly. (For an irregular orbit there is, of course, no question that the exponential growth is transverse.)

Therefore a potentially useful parameter is

$$\gamma = 1 - (A_{ij} \dot{r}_i \dot{r}_j / \dot{r}^2 \text{Tr} A), \quad (25)$$

which does not involve explicitly the time, contrary to α or β . For a periodic orbit γ tends to a limit because one of the eigenvalues of A is considerably larger than the others. We then have $\gamma = \sin^2 \phi$, where ϕ is the angle between $d\vec{r}/dt$ and the major axis of the ellipsoid. For a nonperiodic orbit we likewise expect γ to tend to a limit when we compare points in the vicinity of the original point. This will be illustrated in the following section.

III. NUMERICAL SIMULATIONS

We have applied the proposed test to a large number of orbits of the Hénon-Heiles Hamiltonian²⁰

$$H = (p_x^2 + p_y^2 + x^2 + y^2) / 2 + x^2 y - y^3 / 3, \quad (26)$$

which is extensively documented in the literature. The calculations were performed in double precision (16 digits) with an IBM 370/168 computer. The differential equations were integrated by a Runge-Kutta method (subroutine DVERK of the IMSL library²⁴). The time step was 1/128, which gave results almost identical to a time step of 1/32. To test the accuracy of the calculations we checked the constancy of H (it was conserved to better than one part in 2×10^{10} after a million time steps) and also that $\text{Det}S = 1$ (Liouville's theorem). However, the elements of S are large and the unit determinant results from the small difference of large numbers. Therefore we could only expect to get

$$|\text{Det}S - 1| \ll 10^{-16}(\text{Tr}A)^2,$$

in view of Eq. (22), which was indeed well satisfied. (Incidentally, this shows why $\text{Tr}S$, which oscillates between large positive and negative values, cannot be as good an indicator as $\text{Tr}A$.) The most stringent test of numerical accuracy is shown in Fig. 2. After 3358 turns (a "turn" is the crossing of the $x = 0$ plane with $\dot{x} > 0$) corresponding to $t = 21\,506.3$, the value of y cannot be in error by more than 2×10^{-11} , as a larger error would cause a noticeable misalignment of the points in the graph.

The "vicinity" of the initial point, where we calculated and recorded the values of α , β , and γ , was defined by the following criteria. The point reached at some iteration was deemed "close" to the initial point and recorded if its distance was less than 10^{-2} and also less than (a) the distance at the preceding step, (b) that at the following step,

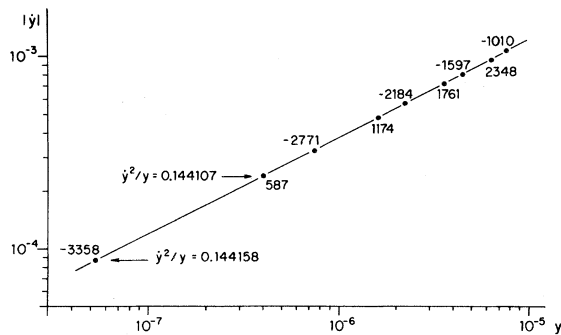


FIG. 2. Surface of section of the D orbit in the vicinity of the initial point $y = \dot{y} = 0$. The ratio y^2/\dot{y} is virtually constant, as expected for a smooth curve. The number of turns required to reach each point has been indicated. Negative serial numbers denote negative \dot{y} . (For the entire oval shaped section, see Fig. 3 of Ref. 20 or Fig. 1 of Ref. 26.)

TABLE I. Initial values of y and \dot{y} for ten orbits.

Orbit	y	\dot{y}
D	0	0
stable periodic	0.302 666 817	0
unstable periodic	-0.185 405 087	0
G	0.07	0.08
E	-0.12	0.1
I	0.35	0.06
K	0.33	0.06
L	0.3318	0.0599
M	0.332	0.059 95
N	-0.011	0

and (c) the last recorded distance multiplied by $e^{\beta T/2}$, where β means the last recorded value of β and T is the time elapsed since that record. The third condition was obviously necessary to give chaotic orbits a chance to pass again in the vicinity of the original point. We did not seek points of closest approach by interpolating between consecutive iterations, because this led to no improvement in the results.

Table I gives the initial y and \dot{y} of the orbits which we investigated. All these orbits had initially $x = 0$ and $\dot{x} > 0$. The value of \dot{x} was given by the energy which was 1/8 for all orbits, except for orbit D , which had energy 1/12. (Orbits D , E , G , and I are the same as in Ref. 25, others have been labeled arbitrarily.)

Orbit D is well known to be regular.^{20,25,26} Its Poincaré surface of section in the vicinity of the origin is given by Fig. 2. The parameters α and γ are nearly constant for $t > 1000$, as shown by Fig. 3. The behavior at the selected points shows none of the oscillations which would be observed if we

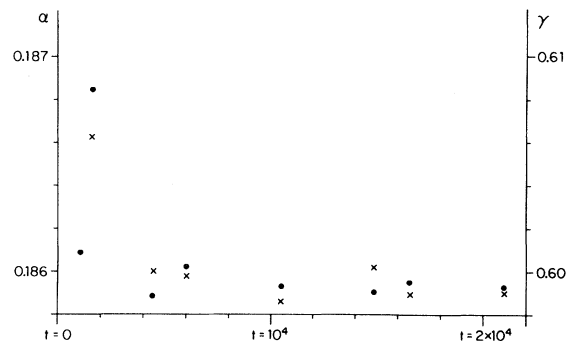


FIG. 3. The parameters α (dots) and γ (crosses) of the regular D orbit are very nearly constant for $t > 1000$. Note that the vertical scales do not start from zero.

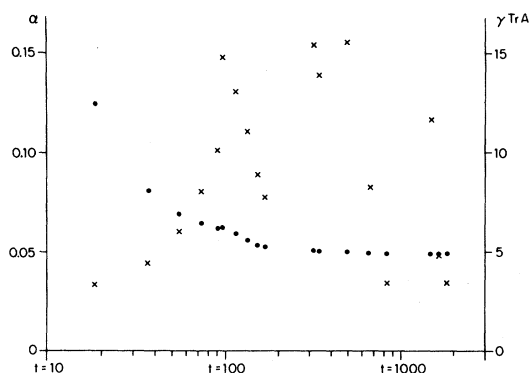


FIG. 4. Stable periodic orbit starting at elliptic fixed point. The parameter α (dots) tends to 0.049 and the transverse cross section of the ellipsoid (proportional to $\gamma \text{Tr}A$, shown by crosses) seems to be bounded, so that $\gamma \rightarrow 0$ as t^{-2} .

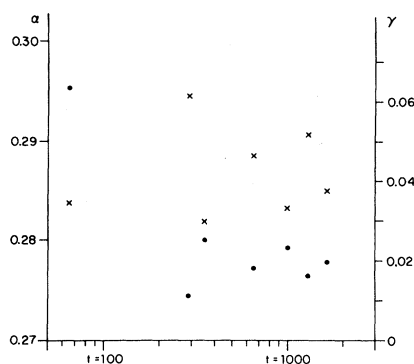


FIG. 6. The parameters α (dots) and γ (crosses) for the regular orbit G . Note that the scale of α does not start from zero.

took constant time intervals (see Fig. 11 of Ref. 16 or Fig. 1 of Ref. 17).

Even more regular results are displayed in Fig. 4 for a stable periodic orbit starting at an elliptic fixed point. The value of α stabilizes after only 200 time units (30 turns) but γ was found to decrease roughly as t^{-2} . We then plotted $\gamma \text{Tr}A$ which, by Eq. (25), gives a measure of the projection of the ellipsoid on a hyperplane orthogonal to $d\vec{r}/dt$. This quantity appears to be bounded, as if the growth of the ellipsoid indeed was parallel to $d\vec{r}/dt$. It is, however, quite possible that a much

longer run would have finally given a nonvanishing limit for γ .

The opposite extreme is Fig. 5, giving β and γ

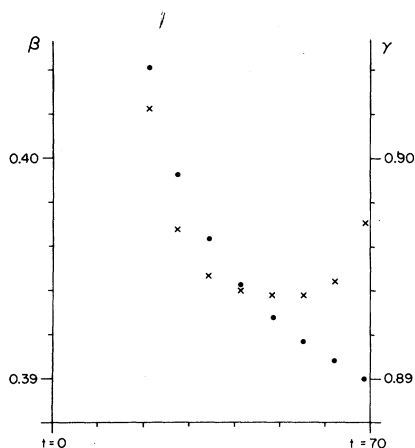


FIG. 5. The parameters β (dots) and γ (crosses) for an unstable periodic orbit starting at a hyperbolic fixed point. Both parameters are fairly constant after only a few turns. Note that the vertical scales do not start from zero.

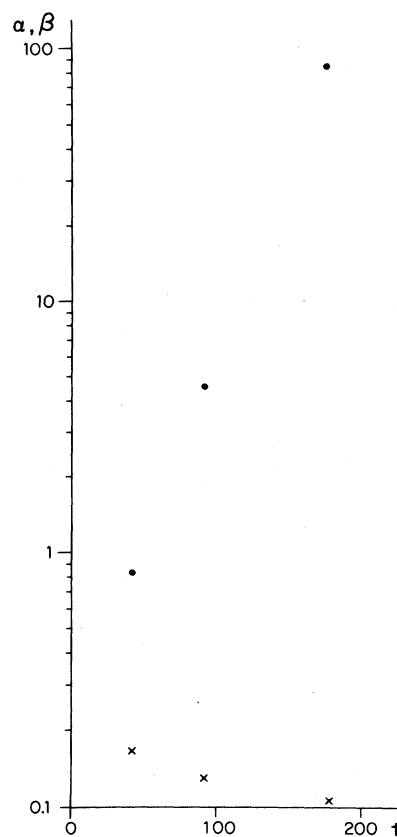


FIG. 7. The parameters α (dots) and β (crosses) for the chaotic orbit E . This orbit was calculated up to $t = 2000$ but did not satisfy the criterion for recording new points in the vicinity of its origin.

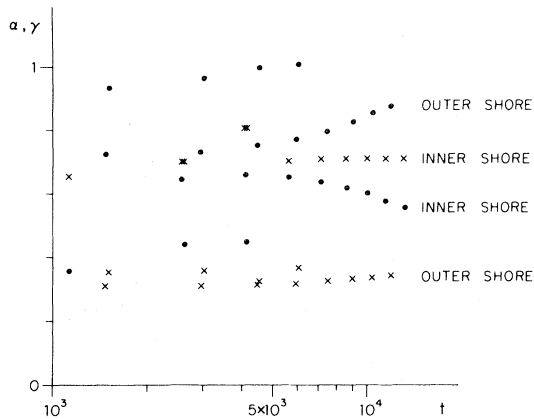


FIG. 8. The parameters α (dots) and γ (crosses) for the regular orbit I . The different limits of α and γ , for $t > 6000$, correspond to different regions of the invariant torus (the outer shore and inner shore of one of the islands of Fig. 9).

for an unstable periodic orbit, starting at a hyperbolic fixed point. Just a few turns are needed to obtain $\beta \approx 0.38$, while γ tends to 1 (the ellipsoid growth is mostly transverse).

We also tested our method with three orbits which are well documented by Powell and Percival.²⁵ Orbit G , which is regular, gave a nearly constant α for $t > 300$, as shown in Fig. 6. On the other hand, orbit E is clearly shown by Fig. 7 to be chaotic. The most interesting case is orbit I , which Fig. 4 of Ref. 25 shows "hesitating" between linear and exponential growth. Our results, shown in Fig. 8, indicate a clearly regular behavior, but α and γ seem to oscillate between two limits. This unexpected behavior becomes clear when we draw

the Poincaré surface of section, Fig. 9. The latter consists of a chain of seven very narrow islands and the initial point is on the "outer shore" of one of them. However, the island is so narrow that part of its "inner shore" is also included in the vicinity of the initial point, as defined by our criteria. If we had more stringent criteria for "vicinity," Fig. 8 would show only *some* of the points belonging to the outer shore, but it would have required a much longer time to collect enough points.

We thus obtained an unexpected bonus from our use of an extended vicinity of the initial point. The multiple limit behavior of α and γ neatly indicates that the invariant torus is not smooth but rather has a complicated shape within this vicinity.

An enlarged view of the gap between two islands is shown in Fig. 10. We have drawn the sections of additional stable orbits, K , L , and M . There must be a hyperbolic fixed point somewhere between them and by further enlarging this area, one would finally obtain a chaotic orbit trapped between the regular orbits K , L , and M . As the latter are extremely close to each other, no drawing (on a reasonable scale) would ever disclose the chaotic nature of this trapped irregular region.

Orbit N shown in Fig. 11 is another example of such a trapped irregular region. Its surface of section looks perfectly regular but the results of our test, given by Fig. 12, unmistakably disclose that it is not. The Lyapunov characteristic number is of course very small, about 0.002. Finally, Fig. 13 shows an enlarged view of the surface of section of orbit N , near its origin. There can be no doubt as to its chaotic nature. The clustering of points suggests that orbit N is in fact very close to some unstable periodic orbit with 232 turns.

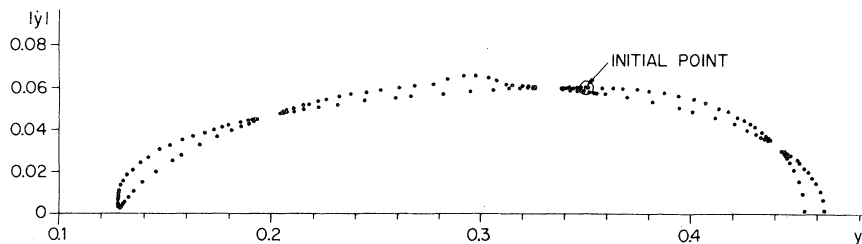


FIG. 9. The I orbit is regular and consists of seven narrow islands. This figure shows all points from 0 to 153 and a few additional ones near the initial point (0.35, 0.06). The small circle around the initial point is the vicinity where we record the shape of the ellipsoid. The coordinates of point 2198 were found (0.349999, 0.060000) so that this is almost a fixed point.

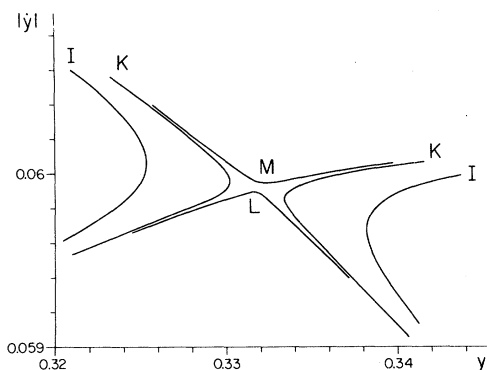


FIG. 10. Enlarged view of the gap between two islands of orbit *I* (see Fig. 9). The surfaces of sections of orbits *K*, *L*, and *M* show that there is a seventh-order hyperbolic fixed point and there must be a chaotic orbit trapped somewhere between these orbits.

IV. CONCLUSION

In this article we have proposed an efficient and relatively easy method to test the stability of a classical Hamiltonian orbit. This method is an improvement of the one which consists in following the separation of neighboring orbits. It is more reliable and accurate, especially in the case of marginal stability. It has the additional advantage of indicating whether or not the invariant torus has a smooth shape in the vicinity of the initial point.

There are two other widely used tests for regularity. One is to draw a Poincaré surface of section and to assess, by visual inspection, whether the points appear to lie on a reasonable curve. As the example of Figs. 11 and 13 show, this method is not reliable in marginal cases such as a narrow

chaotic region trapped between regular tori.

The other test, which we did not use here, is Fourier transforming the motion to find its spectrum.^{25,27,28} Ideally, a regular motion would give a line spectrum with few, strong components; an irregular one would give a complicated spectrum with many weak components. We feel that this test is ambiguous, especially in marginal cases. (An extreme counterexample is an unstable *periodic* orbit, such as the one of Fig. 5, which must have a very simple line spectrum.)

It is of course possible to imagine marginal cases for which no method yields a result within a preset time. However, in most cases, the method describing in this article can yield a clear answer with a high degree of reliability.

Note added. The linear separation rate of regular orbits was proved by Casati *et al.*²⁹ for integrable Hamiltonians (our proof is less direct, but does not require integrability). There are, however, “pseudo-integrable” Hamiltonians for which *infinitesimally* close orbits separate linearly, but are nevertheless chaotic. The simplest example is a polygonal enclosure^{30,31} where the chaotic property does not arise from the exponential divergence of neighboring trajectories, but from their occasionally hitting the polygon on different sides of a vertex. Our stability test, which tacitly assumes differentiable potentials, is not applicable to these cases.

ACKNOWLEDGMENTS

We are grateful to M. V. Berry and I. C. Percival for helpful comments. This work was sup-

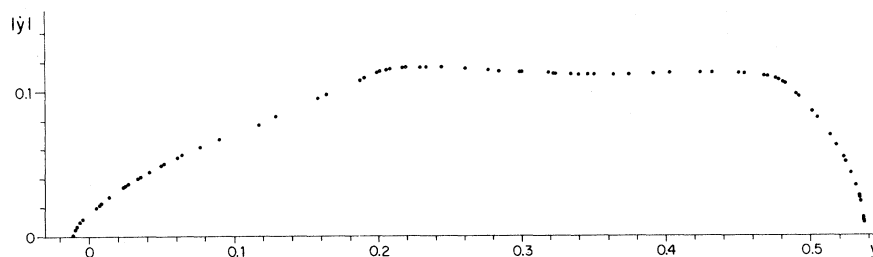


FIG. 11. Surface of section of orbit *N*. The figure shows all points from 0 to 51 and 24 additional points in selected areas. This orbit seemed regular when drawn with a reasonable scale (1 unit = 1 meter) but is in fact chaotic, as shown in Fig. 13.

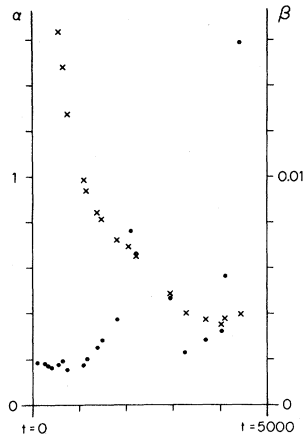


FIG. 12. The parameters α (dots) and β (crosses) for orbit N . For $t < 1000$, the behavior seems regular ($\alpha \rightarrow \text{const}$) but for $t > 3000$ we clearly see that it is chaotic ($\beta \rightarrow \text{const}$).

ported in part by the Gerard Swope Fund and the VPR Fund for Research. We are also grateful to J. Ford for drawing our attention to Refs. 29–31.

APPENDIX A: EIGENVALUES OF REAL SYMPLECTIC MATRICES

In this appendix, we show that the eigenvalues of S are paired as λ and λ^{-1} and, in particular, complex eigenvalues lie on the unit circle. Let \vec{v} be an eigenvector of S belonging to the eigenvalue λ . We have $S^{-1}\vec{v} = \lambda^{-1}\vec{v}$ and thus, by Eq. (12),

$$\tilde{S}\eta\vec{v} = \eta\tilde{S}^{-1}\vec{v} = \lambda^{-1}\eta\vec{v}. \quad (\text{A1})$$

Therefore $\eta\vec{v}$ is an eigenvector of \tilde{S} belonging to the eigenvalue λ^{-1} . But S and \tilde{S} have the same eigenvalues (since they have the same characteristic equation), therefore all these eigenvalues are paired: λ and λ^{-1} .

Moreover, since S is real, its complex eigenvalues are also paired as λ and λ^* . We now show that this must be the *same* pairing as before, i.e., we cannot have four *distinct* eigenvalues z , z^* , z^{-1} , and z^{*-1} . Indeed, from $S\vec{v}^* = z^*\vec{v}^*$ and (A1) we have

$$\vec{v}^*\tilde{S}\eta\vec{v} = z^*\vec{v}^*\eta\vec{v} = z^{-1}\vec{v}^*\eta\vec{v}, \quad (\text{A2})$$

where \vec{v} denotes the transposed of \vec{v} . If $\vec{v} \neq \vec{v}^*$, then $\vec{v}^*\eta\vec{v}$ is generally not zero, so that $z^* = z^{-1}$.

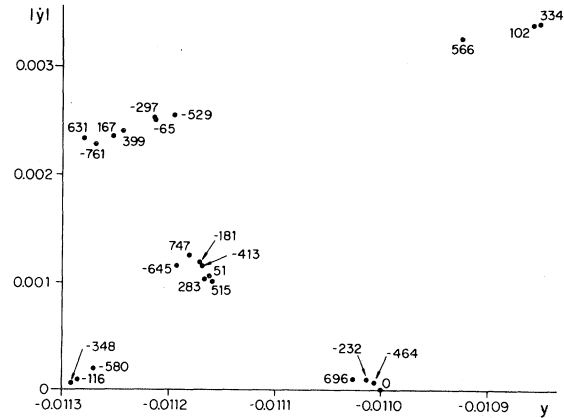


FIG. 13. The origin of orbit N seen “under a microscope.” Points with negative serial numbers are those with negative \dot{y} . The chaotic nature of the orbit is conspicuous. The clustering of points shows that it is very close to a periodic orbit with 232 turns.

APPENDIX B: A CANONICALLY INVARIANT METHOD

As explained at the end of the Introduction, notions such as distance, sphere, angle, etc., imply the use of a Euclidean metric in phase space, which cannot be canonically invariant. It is possible to reformulate our test in a way which makes no use of a Euclidean metric (and therefore makes no appeal to geometrical intuition) but is manifestly invariant under canonical transformations.

Indeed, an expression such as

$$Z = \rho_j \left[\frac{\partial^2 H}{\partial r_j \partial r_k} \right] \rho_k = \frac{d\vec{\rho}}{dt} \eta \vec{\rho}, \quad (\text{B1})$$

is canonically invariant. (The simpler expression

$$\frac{d\vec{r}}{dt} \eta \vec{\rho} = \left[\frac{\partial H}{\partial r_i} \right] \rho_i, \quad (\text{B2})$$

cannot be used for this purpose because it is constant by energy conservation.) It is then found that for a regular orbit, Z increases *quadratically* with time, and for a chaotic orbit, Z increases exponentially.

This result is independent of the initial choice of $\vec{\rho}$ (except for a set of measure zero) because almost any $\vec{\rho}$ will tend to align itself parallel to the longest axis of the ellipsoid defined in Sec. II.

*Now at RAS-CAL Ltd., Safed, Israel.

- ¹*Stochastic Behavior in Classical and Quantum Hamiltonian Systems*, Volta Memorial Conf., Como 1977, edited by G. Casati and J. Ford (Springer, Berlin, 1979).
- ²*Topics in Nonlinear Dynamics (LaJolla Institute)*, Proceedings of the Workshop on Topics in Nonlinear Dynamics, AIP Conference Proceeding No. 46, edited by S. Jorna (AIP, New York, 1978).
- ³*Proceedings of the Symposium on Nonlinear Dynamics and the Beam-Beam Interaction*, AIP Conference Proceedings No. 57, edited by M. Month and J. C. Herrera (AIP, New York, 1979).
- ⁴K. J. Whiteman, Rep. Prog. Phys. **40**, 1033 (1977).
- ⁵R. Bellman, *Stability Theory of Differential Equations* (McGraw-Hill, New York, 1953).
- ⁶G. Contopoulos, Astrophys. J. **138**, 1297 (1963).
- ⁷F. G. Gustavson, Astron. J. **71**, 670 (1966).
- ⁸Y. M. Treve, Ref. 2, pp. 147–220.
- ⁹I. C. Percival, Ref. 1, pp. 259–282.
- ¹⁰B. V. Chirikov, J. Ford, and F. Vivaldi, Ref. 3, pp. 323–340.
- ¹¹C. Froeschlé and J. -P. Scheidecker, Phys. Rev. A **12**, 2137 (1975).
- ¹²M. V. Berry, Ref. 2, pp. 16–120.
- ¹³J. M. Greene, J. Math. Phys. (N.Y.) **2**, 760 (1968); **20**, 1183 (1979).
- ¹⁴Ja. G. Sinai and E. B. Vul, J. Stat. Phys. **23**, 27 (1980).
- ¹⁵R. H. G. Helleman and T. Bountis, Ref. 1, pp. 353–375.
- ¹⁶J. Ford and G. H. Lunsford, Phys. Rev. A **1**, 59 (1970).
- ¹⁷G. Casati and J. Ford, Phys. Rev. A **12**, 1702 (1975).
- ¹⁸G. Benettin, L. Galgani, and J. -M. Strelcyn, Phys. Rev. A **14**, 2338 (1976).
- ¹⁹G. Benettin, C. Froeschlé, and J. -P. Scheidecker, Phys. Rev. A **19**, 2454 (1979).
- ²⁰M. Hénon and C. Heiles, Astron. J. **69**, 73 (1964).
- ²¹N. L. Balazs, Physica **A102**, 236 (1980).
- ²²M. Hamermesh, *Group Theory* (Addison-Wesley, Reading, Mass., 1962).
- ²³B. V. Chirikov, Phys. Rep. **52**, 263 (1979).
- ²⁴IMSL library reference manual, 8th ed. (IMSL Inc., Houston, Texas, 1980).
- ²⁵G. E. Powell and I. C. Percival, J. Phys. A **12**, 2053 (1979).
- ²⁶G. Walker and J. Ford, Phys. Rev. **188**, 416 (1969).
- ²⁷D. W. Noid, M. L. Koszykowski, and R. A. Marcus, J. Chem. Phys. **27**, 404 (1977).
- ²⁸S. Blacher and J. Perdang, Physica D **3**, 512 (1981).
- ²⁹G. Casati, B. V. Chirikov, and J. Ford, Phys. Lett. **77A**, 91 (1980).
- ³⁰A. N. Zemlyakov and A. B. Katok, Mat. Zametki **18**, 291 (1975) [Math. Notes **18**, 760 (1976)].
- ³¹P. J. Richens and M. V. Berry, Physica **2D**, 495 (1981).